Available online at www.sciencedirect.com
ScienceDirect
Polymer 48 (2007) 7374–7384
polymer
www.elsevier.com/locate/polymer

# Crystallization behavior and mechanical properties of polypropylene/halloysite composites

Nan-ying Ning, Qin-jian Yin, Feng Luo, Qin Zhang, Rongni Du, Qiang Fu*

*Department of Polymer Science and Materials, State Key Laboratory of Polymer Materials Engineering, Sichuan University, Chengdu 610065, People's Republic of China*

Received 23 June 2007; received in revised form 6 September 2007; accepted 8 October 2007
Available online 12 October 2007

**Abstract**

In this work, halloysite nanotubes (HNTs), a new type of inexpensive filler, were used for the modification of polypropylene (PP). HNTs were first surface treated by methyl, tallow, bis-2-hydroxyethyl, quaternary ammonium, then melt mixed with PP. Scanning electron microscope (SEM) was used to examine the dispersion of HNTs in PP matrix. Differential scanning calorimetry (DSC), polarized light microscope (PLM), dynamic melt rheometry and wide angle X-ray diffraction (WAXD) were employed to investigate the crystallization behavior of the prepared PP/HNT composites. The mechanical properties were evaluated by Instron and impact tests. SEM results revealed that HNTs could be well-dispersed in PP matrix and had a good interfacial interaction with PP, even up to a high content of 10 wt%. DSC data indicated that HNTs could serve as a nucleation agent, resulting in an enhancement of the overall crystallization rate and the non-isothermal crystallization temperature of PP. PLM showed a constant spherulite growth rate and a decreased spherulite size at given isothermal crystallization temperature, suggesting that nucleation and growth of a spherulite are two independent processes. The result obtained by dynamic melt rheometry indicated that HNTs mainly promoted nucleation and had not much influence on the growth of PP crystallization. Nevertheless, by fast cooling the samples, almost constant spherulite size can be obtained for both pure PP and PP/HNT composites due to the limited nucleation effect of HNTs on PP crystallization. WAXD showed that HNTs mainly facilitated α-crystal form of PP. Though a good dispersion of HNTs in PP matrix was observed, out of our expectation, not much enhancement on mechanical properties of PP/HNT composites had been achieved, and this could be mainly ascribed to the constant crystallinity and spherulite size of PP as well as the small length/diameter ratio of HNTs.


*Keywords:* Polypropylene (PP); HNTs; Crystallization behavior

## 1. Introduction

Isotactic polypropylene is widely used in industry due to its well balanced physical and mechanical properties and its easy processability at a relatively low cost [1]. However, its relatively poor impact strength restricts its application as an engineering thermoplastic [2]. Therefore, a great deal of work has been done to overcome its disadvantages in the past several decades. On one hand, various kinds of PP copolymers or blends with other polymers have been developed [3–5]. On the other hand, PP has been modified by melt mixing with various kinds of inorganic fillers, such as talc, mica, clay, whiskers, glass fiber, carbon fiber, silica nanoparticles, carbon nanotubes and calcium carbonate ($CaCO_3$) [6–17]. Weawkamol and coworkers [16] observed an increased modulus of PP/nonpurified single wall carbon nanotube (SWNT) composites by 75% at 0.5 wt% SWNTs. In our earlier work [17], we found that the impact strength of PP/clay nanocomposites prepared by melt intercalation was greatly improved, while the tensile strength was not much improved compared with pure PP. As reported by Chan et al. [14], the Izod impact strength of PP/$CaCO_3$

* Corresponding author.
*E-mail address:* qiangfu@scu.edu.cn (Q. Fu).

0032-3861/$ - see front matter © 2007 Elsevier Ltd. All rights reserved.
doi:10.1016/j.polymer.2007.10.005

nanocomposites could be significantly increased by 300%, while the ultimate tensile strength kept relatively constant. Since the physical and mechanical properties of semicrystalline polymers strongly depend on the crystalline morphology, extensive studies on the nucleation activity of fillers, the effect of fillers on the crystallization kinetics, the spherulite growth of polymers and crystalline morphology of composites, as well as the correlation between crystalline structure and mechanical properties of filler-modified PP have been carried out by many researchers [18–24].

Recently, halloysite has received much attention. It is an important member of kaolin group of clay minerals and has a composition of $Al_4Si_4O_{10}(OH)_8 \cdot 4H_2O$. It exhibits hollow nanotubular structure and its typical dimension is of nanoscale. The cost of HNTs is much lower than other nanofillers such as carbon nanotubes. They are usually applied in the manufacture of high quality ceramic white-ware and can also be used as a microtubular drug delivery system, nanotemplates or nanoscale reaction vessles [25–28]. Wu [29] has recently studied HNT/epoxy (EP) composites and observed that HNTs could obviously improve the mechanical properties of EP. Du et al. [30] first utilized HNTs as nanofiller for PP and found that HNTs were well-dispersed in PP matrix at nanoscale after facile modification and the thermal stability of the composites was obviously enhanced compared with pure PP. NaturalNano, Inc. has announced the successful pilot-scale dispersion of functionalized halloysite nanotubes in polypropylene. However, the mechanical properties and crystallization behavior of PP/HNT composites have not been reported yet.

In this work, HNTs were first surface treated by methyl, tallow, bis-2-hydroxyethyl, quaternary ammonium and then melt mixed with PP. Since the morphology and crystallization behavior are directly related to the properties of polymer composites, we focus our attention mainly on the crystallization behavior and mechanical properties of the prepared PP/HNT composites. Different from usual situations, out of our expectation, although HNTs are well-dispersed in PP matrix in a range of 50–300 nm and have a good interfacial interaction with PP, the addition of HNTs can only enhance the crystallization temperature and overall crystallization rate of PP to a certain extent, leading to almost constant spherulite size for pure PP and PP/HNT composites by fast cooling the samples. This may contribute partially to the unchanged mechanical properties observed in the composites.

## 2. Experimental section

### 2.1. Materials

A commercially available isotactic PP was manufactured by Dushanzi Petroleum Chemical Incorporation (Xinjiang, China), with a melt flow index of 0.96 g/10 min (190 °C, 2.16 kg). Halloysite (degree of purity: >90% to 92%) was obtained from Guizhou Province in China. Methyl, tallow, bis-2-hydroxyethyl, quaternary ammonium solution, which was purchased from Bailingwei Chemical Incorporation (Beijing, China), was used as surfactant and the molecular structure ($n = 14–18$) is shown as follows:

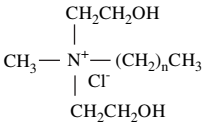

### 2.2. Modification

Naturally occurred halloysite clay purchased from Guizhou Province in China was ground into powder by a laboratory ball mill. The powder was sieved by passing through a 150-mesh stainless steel sifter and then immersed in 5% $K_2CO_3$ solution for 3 days. After filtration, the halloysite residue was treated in 5% methyl, tallow, bis-2-hydroxyethyl, quaternary ammonium solution at 80 °C for 24 h. Then, the suspended substance of halloysite was filtered again. After that, the leavings were dried in a vacuum oven at 60 °C for 24 h. The dried powder was ground by a laboratory ball mill again and was sieved by passing through a 150-mesh stainless steel filter. The ultimate powder was used as nanofiller, as shown in Fig. 1.

### 2.3. Preparation of PP/HNT composites

PP and HNTs were melt mixed using a twin screw extruder. The temperature of the extruder was maintained at 150 °C, 190 °C, 190 °C, 200 °C, 200 °C and 190 °C from hopper to die, and the screw speed was 110 rpm. Pure PP was also passed through extruder under the same conditions to serve as a reference. The pelletized granules were dried for 20 h under 80 °C and then injection molded under the temperature of 200 °C. The ultimate PP/HNT (with different modified HNT content of 1 wt% and 10 wt%) samples were termed as 1HPP and 10HPP, respectively.

### 2.4. Scanning electron microscopy (SEM)

The morphologies of HNTs and PP/HNT composites were examined under an acceleration voltage of 20 kV with a JEOL

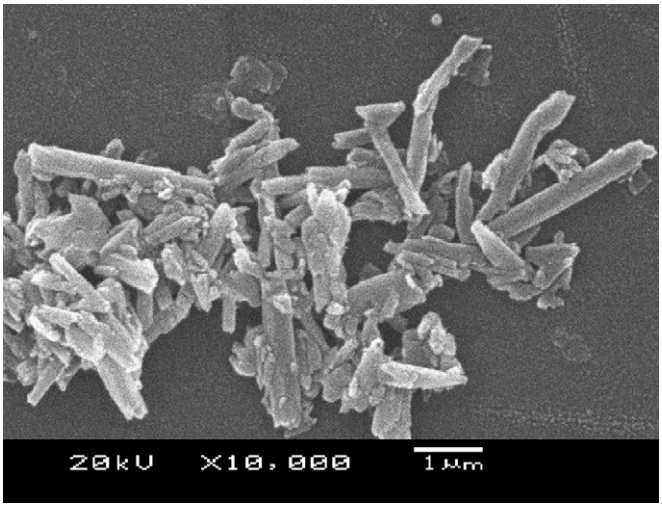


Fig. 1. SEM photo of HNTs.

JSM-5900 LV for SEM experiment. Before being examined, the specimens of PP/HNT composites were cryogenically fractured perpendicular to the flow direction in liquid nitrogen (−170 °C) and then the fractured surface was coated with a thin layer of gold.

### 2.5. Differential scanning calorimetry (DSC)

A Perkin–Elmer pyris-1 DSC with nitrogen as purge gas was used to investigate the crystallization behavior of pure PP and PP/HNT composites. In the case of isothermal crystallization, the samples (about 5.0 mg) were heat-treated at 200 °C for 5 min in order to eliminate any thermal history. Then they were cooled at a rate of 100 °C/min to the crystallization temperature, $T_c$, and maintained at that temperature during the time for complete crystallization of the matrix. The heat evolved during isothermal crystallization was recorded as a function of time. The isotherms were constructed by integrating the area under the exothermic peak. Then the specimens were heated again without prior cooling to obtain the DSC endotherms at a rate of 10 °C/min. The melting temperatures ($T_m$s) were determined from the maxima of the fusion peaks. The crystallinity ($X_c$) of the blends was calculated from the equation $X_c = \Delta H_i/(\varphi_i \Delta H_i^m)$, where $\Delta H_i$ is the enthalpy of fusion of 1HPP or 10HPP, directly obtained by DSC, and $\varphi_i$ is the mass fraction of PP in the blends. $\Delta H_i^m$, the enthalpy of fusion of 100% crystalline polymer, is 209 J/g for PP [31]. The non-isothermal crystallization behavior of the specimens was investigated by melting the samples (about 5 mg) at 200 °C for 5 min to erase any thermal history and prevent self-seeding of PP and then cooling them to 30 °C at a cooling rate of 10 °C/min. Thereafter, the specimens were heated again to the melting point at a heating rate of 10 °C/min.

### 2.6. Polarized light microscope (PLM)

A polarized light optical microscope equipped with a hot stage was used to study the crystallization morphology and the isothermal spherulite growth rate of neat PP and composites. The samples sandwiched between two microscope cover slips were first heated to 200 °C, pressed into thin film samples, and then maintained at 200 °C for 5 min. The temperature of the hot stage was then reduced to the fixed crystallization temperature ($T_c$) at a rate of 100 °C/min. The crystallization process was observed and the morphologies were recorded by taking photographs at constant time intervals. The radial growth rate of spherulites was determined by measuring the radii of the growing spherulites as a function of time. The non-isothermal crystallization morphology was obtained by melting the samples at 200 °C for 5 min to erase any thermal history and then cooling them at 50 °C/min to the room temperature. Reported results were averages of at least three fresh samples.

### 2.7. Dynamic melt rheometry

The crystallization behavior under shear was studied by rheological measurement, which was performed on a controlled strain rheometer (ARES rheometer, Rheometrics Scientific, NJ) with a torque transducer range of 0.2–2000 gf cm using 25 mm diameter parallel plates. Testing sample disks with a thickness of 1.5 mm and a diameter of 25 mm were prepared by compression molding of the extruded pellets at 190 °C for 3 min. Pure PP and PP/HNT composites were examined in dynamic time sweep mode at an angular frequency of 1 Hz and 0.1% strain level. The temperature of the samples was raised to 200 °C and held at that temperature for 5 min to eliminate any thermal history, and then lowered to the desired crystallization temperature of 132 °C at a cooling rate of 30 °C/min. All measurements were conducted under a nitrogen atmosphere to minimize oxidative degradation of PP.

### 2.8. Wide angle X-ray diffraction (WAXD)

WAXD analysis was conducted with a DX-100 X-ray diffractometer (radiation Cu K$\alpha$, $\lambda = 0.154$ nm, reflection mode) at room temperature. The $2\theta$ range is 10°–25° with a scanning rate of 0.05°/s. The testing samples were prepared by compression molding of the extruded pellets at 190 °C for 3 min. The crystallinity was calculated from diffracted intensity data over the range from 10° to 25° of $2\theta$ by using the area integration method [32].

### 2.9. Mechanical properties

Standard tensile tests were performed using an Instron universal tensile testing machine with a cross-head speed of 50 mm/min at room temperature (23 °C). The width and thickness of the dumbbell shaped specimens were about 10.20 mm and 4.24 mm. The tensile strength at yield was determined according to GB/T 1040-92 standard.

For impact strength measurement, a notch with 45° was made by machine, and the remaining width of the specimens was 8.0 mm. The notched Izod impact strength of the specimens was tested with a VJ-40 Izod machine, according to GB/T 1834-1996 standard. The values of all the mechanical parameters were calculated as averages over 5 specimens for each composition.

## 3. Results

### 3.1. Morphology of HNTs and its dispersion in PP/HNT composites

The SEM micrograph, as shown in Fig. 1, reveals the nanotubular structure of halloysite. Many agglomerates and a few particles can also be seen. The typical diameter and length/diameter ratio of HNTs are determined by measuring 10 randomly chosen nanotubes. However, it is difficult to determine the primary size of HNTs precisely due to aggregate nature of the nanotubes. The diameter ranges from 50 nm to 300 nm and the length/diameter ratio is in the range of 3–10.

It is well-known that the dispersion of filler in polymer matrix is a key for the enhancement of mechanical properties of polymer composites. Generally, it is difficult to achieve a good

dispersion of inorganic filler in a thermoplastic. And this problem is even worse as the nanoparticles are used, due to the strong tendency of filler agglomeration [14]. However, in our work, the modified HNTs are seen to be well-dispersed in PP matrix, even at a high filler content of 10 wt%, as shown in Fig. 2. It can be seen that a good dispersion is achieved for all the composites containing 1 wt% and 10 wt% HNTs and no aggregate can be found. Most of the HNTs are uniformly dispersed in PP matrix with a size between 50 nm and 300 nm. The interface of PP and HNTs is blurrier and no obvious cavities can be seen, suggesting a good interfacial interaction between the modified HNTs and PP matrix.

### 3.2. DSC results

In Fig. 3(a), different curves are presented concerning the isothermal crystallization process at 128 °C for pure PP and PP/HNT composites. From this figure, it is deduced that the addition of HNTs has an effect on the enhancement of the overall crystallization rate of PP, which becomes faster by adding HNTs. Since the half crystallization time $t_{1/2}$ (defined as the time required to reach 50% of the complete crystallization) is a very important parameter describing the overall crystallization rate, the $t_{1/2}$ values obtained for PP/HNT composites and pure PP specimens are plotted against $T_c$ values, as shown in Fig. 3(b). It can be seen that the overall crystallization rate for the samples decreases with increasing crystallization temperature as it increases from 125 °C to 132 °C. However, the crystallization rate increases ($t_{1/2}$ decreases) with the increase of HNT content at the same $T_c$, mainly at high $T_c$. For example, the $t_{1/2}$ of PP at 132 °C is about 966 s, which is decreased to 468 s for 10HPP at the same crystallization temperature. This result suggests that HNTs can serve as a heterogeneous nucleation agent for PP crystallization. Furthermore, the melting temperature is found to be almost the same for all the samples if they are crystallized at the same temperature. For example, the melting traces of pure PP and PP/HNT composites crystallized at 128 °C are shown in Fig. 3(c). Obviously, no significant changes in the full width of the melting peaks or the melting temperatures are detected between the samples. It can be deduced that the crystallite size distribution of PP is hardly changed with the presence of HNTs. Fig. 4 shows the crystallinity of pure PP and PP/HNT composites crystallized at various temperatures. It can be seen that the crystallinity of all the specimens increases slightly with the enhancement of crystallization temperature. One can also observe a constant crystallinity (about 33%) within the experimental error for all the specimens crystallized at the same temperature, which indicates that the addition of HNTs has no obvious effect on the crystallinity of PP.

The effect of HNTs on the crystallization behavior of PP can also be demonstrated by non-isothermal crystallization. As an example, the non-isothermal crystallization curves of pure PP and PP/HNT composites at a cooling rate of 10 °C/min are shown in Fig. 5(a). The crystallization peak temperature is defined as $T_p$. It can be seen that $T_p$ shifts to higher temperature with the presence of HNTs. This result indicates

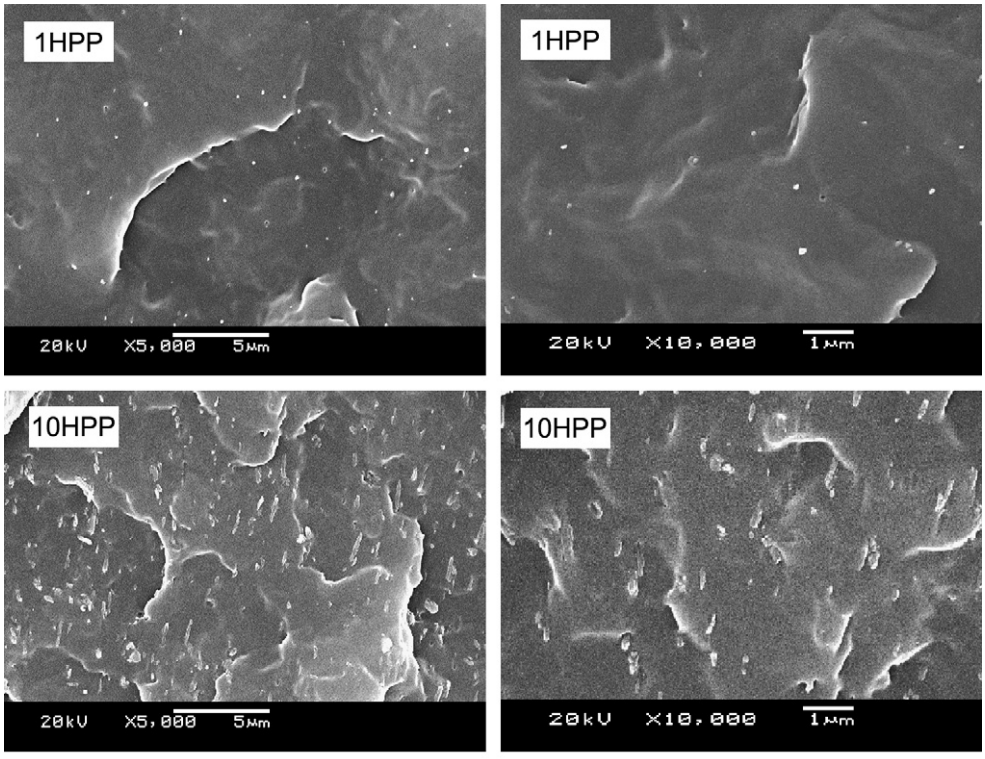


Fig. 2. SEM photos of fracture surface of PP/HNT composites (a) ×5000 and (b) ×10 000.

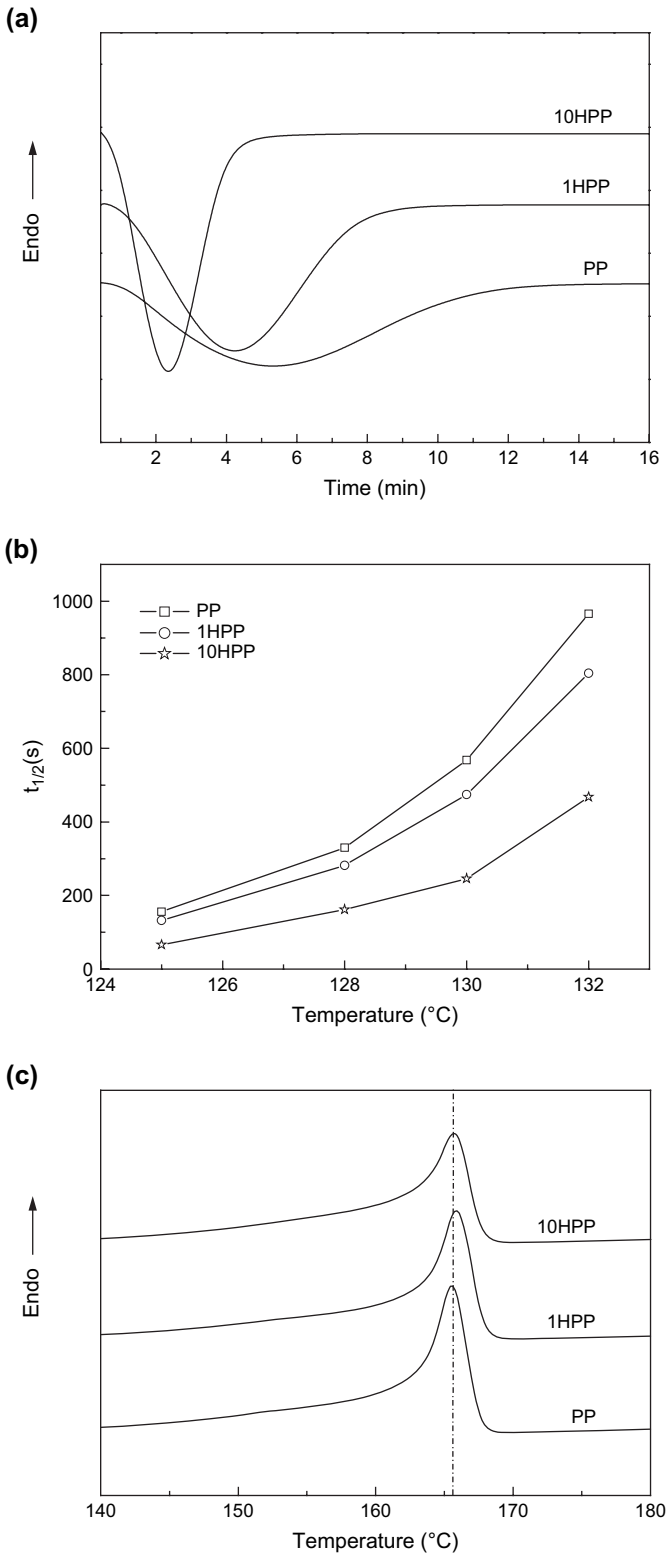


Fig. 3. Isothermal crystallization and melting behavior of pure PP and PP/HNT composites. (a) Isothermal crystallization isotherms (crystallized at 128 °C), (b) half crystallization time ($t_{1/2}$) versus crystallization temperatures, and (c) melting traces (heating rate: 10 °C/min, crystallized at 128 °C).

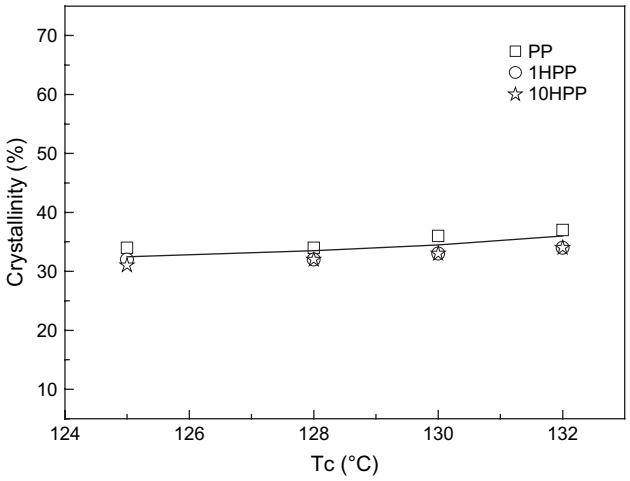


Fig. 4. Crystallinity of pure PP and PP/HNT composites crystallized at various temperatures.

again the efficiency of HNTs as a nucleating agent for PP crystallization, but mainly at high HNT content. The corresponding heating curves are shown in Fig. 5(b), and again almost constant melting temperature is observed. These results are in good agreement with the above isothermal crystallization results.

Nevertheless, it should be noted that the nucleation effect of HNTs on PP crystallization is limited compared with other good nucleation agent of PP reported in the literature. For example, Seo et al. [1] investigated the crystallization kinetics of PP/MWNT composites and observed that the addition of 1 wt% MWNTs increased the crystallization rate by as much as an order of magnitude or higher and the addition of 5 wt% MWNTs increased the $T_p$ by 12 °C. However, in PP/HNT composites, the enhancement of $T_p$ is only 5 °C even for 10HPP and the overall crystallization rate is only twice that of pure PP when crystallized at 132 °C, indicating that the nucleation effect of HNTs is limited.

### 3.3. PLM observation

The crystal morphology and the spherulite radial growth rate of PP, 1HPP and 10HPP are examined by PLM. Fig. 6 presents crystal morphology of the samples crystallized at the same temperature (128 °C) at the time of 90 s (left) or 135 s (right). The birefringent spherulitic structure and the same average spherulite size can be observed for pure PP, 1HPP and 10HPP at the same crystallization time. One can also see from this figure that the number of spherulites increased due to the addition of HNTs. This can be ascribed to the nucleation effect of HNTs. The spherulite radial growth rates of PP/HNT composites and pure PP are carefully investigated at a variety of crystallization temperatures and time. As an example, the spherulite radius as a function of crystallization time for the specimens crystallized at 128 °C is plotted in Fig. 7. One observes a linear increase of the spherulite size with time for all the samples before the impingement of spherulites. Fig. 8 shows the spherulite radial growth rate ($G$) of PP and PP/

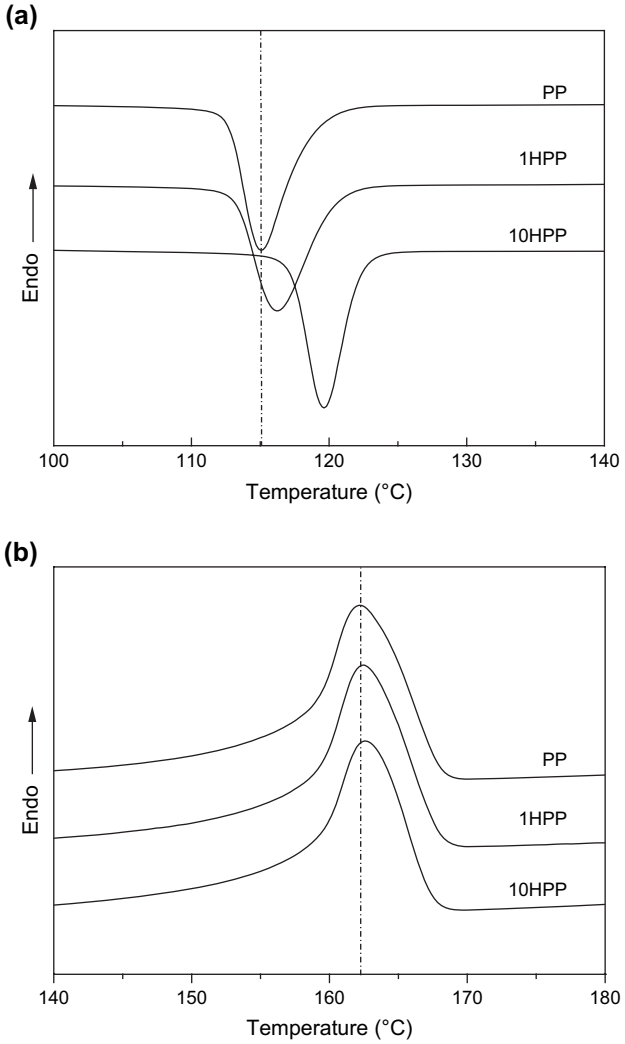


Fig. 5. Non-isothermal crystallization and melting traces of pure PP and PP/HNT composites. (a) Crystallization exotherms (cooling rate: 10 °C/min) and (b) melting traces (heating rate: 10 °C/min).

HNTs at various crystallization temperatures. It can be seen that the spherulite radial growth rate decreases with increasing crystallization temperature for all the specimens, suggesting a nucleation-controlled growth. Again, the spherulite growth rate of PP, within the experimental error, is not affected by the incorporation of HNTs at each temperature studied. Thus, it becomes clear that the reason of enhancement of the overall crystallization rate (obtained by DSC results) is due to the presence of HNTs as a nucleation agent, and has nothing to do with the spherulite growth rate. These results indicate that nucleation and growth of a spherulite are two independent processes for the composites studied in this paper.

The final spherulite size of the samples obtained by isothermal crystallization at a relatively high temperature will depend on the density of nucleus. Due to the enhancement of nucleation by adding HNTs, the spherulite in the composites will impinge at an early time thus could end up in a smaller spherulite size, compared with pure PP. As shown in Fig. 9, the final morphology of the three samples is obtained by isothermal crystallization at 128 °C. The spherulite diameter is roughly 300 μm, 210 μm and 150 μm, for PP, 1HPP and 10HPP, respectively. And the corresponding spherulite impingement time is about 11.5 min, 8 min and 5 min, respectively. However, by fast cooling (50 °C/min) the samples from the melt, which is more closer to the real processing conditions, almost the same spherulite size is obtained for PP, 1HPP and 10HPP, as shown in Fig. 10. As we know that the relatively low temperature will benefit the homogeneous nucleation and the role of filler as a nucleation agent will be less effective. Thus, it can be deduced that the density of nucleus in pure PP is almost the same as in PP/HNT composites in this kind of situation and the spherulite growth rate becomes the dominant factor in determining the final spherulite size of the samples. Therefore, it is reasonable to obtain the nearly unchanged spherulite size for PP, 1HPP and 10HPP by fast cooling the samples. Again, it can be concluded that the nucleating effect of HNTs on PP crystallization is not very good in comparison with other effective nucleating agent reported in the literature. As reported by Chan et al. [14], the spherulite size of pure PP is larger than 40 μm while no spherulitic structure can be seen with the incorporation of 9.2 vol% $CaCO_3$ nanoparticles, indicating the excellent nucleating effect of $CaCO_3$ nanoparticles on PP crystallization by dramatically increasing the number of spherulites and significantly reducing the size of spherulites.

### 3.4. Dynamic melt rheometry

In recent years, dynamic melt rheometry has been proved to be a reliable technique to study the crystallization kinetics of polymer materials [33–35]. Khanna [36] has studied the crystallization kinetics of different materials with and without nucleating agent and has shown that the rheological technique was more sensitive than the conventional ones, such as DSC, PLM or X-ray. In addition, he has proposed a relation to deduce the relative crystallinity $\alpha(t)$ based on the rheological measurements:

$$\alpha(t) = \frac{G'(t) - G'(0)}{G'(\infty) - G'(0)} \tag{1}$$

where $G'(0)$, $G'(t)$ and $G'(\infty)$ are the elastic moduli at time 0, $t$ and infinity, respectively. The same type of relation has also been proposed by Gauthier et al. [37]. They have used the rheological measurements to follow the crystallization of poly(ethylene terephthalate)/glass fiber samples and have shown that not only the crystallization kinetics but also the nucleation and growth characteristics could be evaluated by the evolution of storage modulus.

A plot of storage modulus ($G'$) versus time at a given isothermal crystallization temperature (132 °C) for pure PP, 1HPP and 10HPP is shown in Fig. 11. In this plot, one can clearly observe a three-step evolution of storage modulus ($G'$) versus time during crystallization for the three samples. Firstly, $G'$ initially increases monotonically with time, which is referred to as the induction stage of nucleation. Secondly, $G'$ abruptly increases with time, indicating that the crystallites

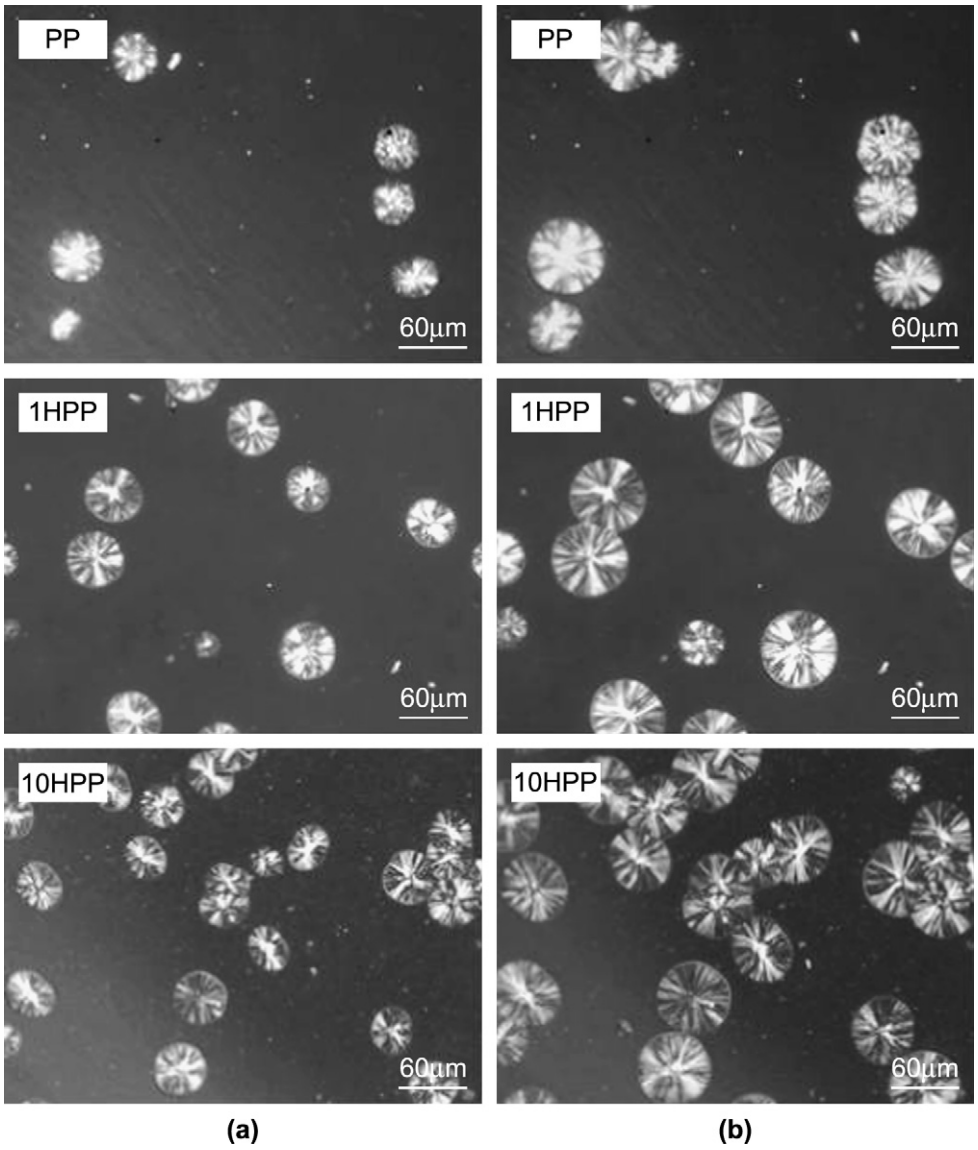


Fig. 6. The crystal morphology of PP/HNT composites as well as pure PP crystallized at 128 °C. Crystallization time is (a) 90 s and (b) 135 s.

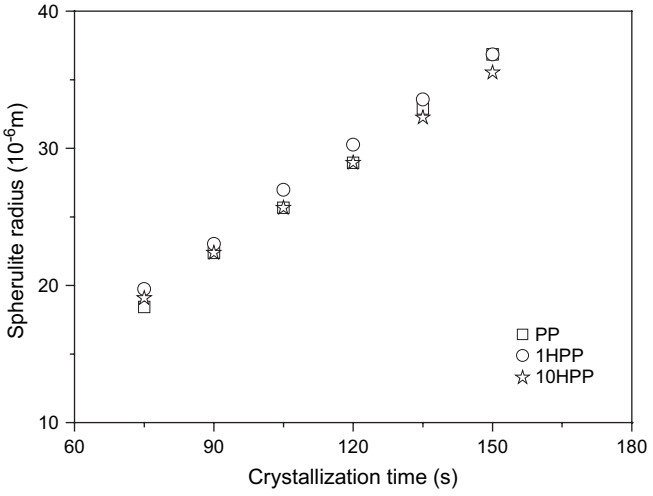


Fig. 7. Spherulite radius versus time of pure PP and PP/HNT composites crystallized at 128 °C.

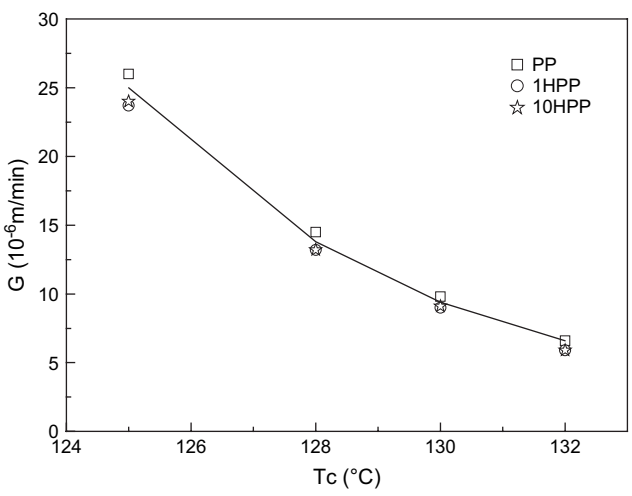


Fig. 8. Spherulite grow rate of pure PP and PP/HNT composites at various crystallization temperatures.

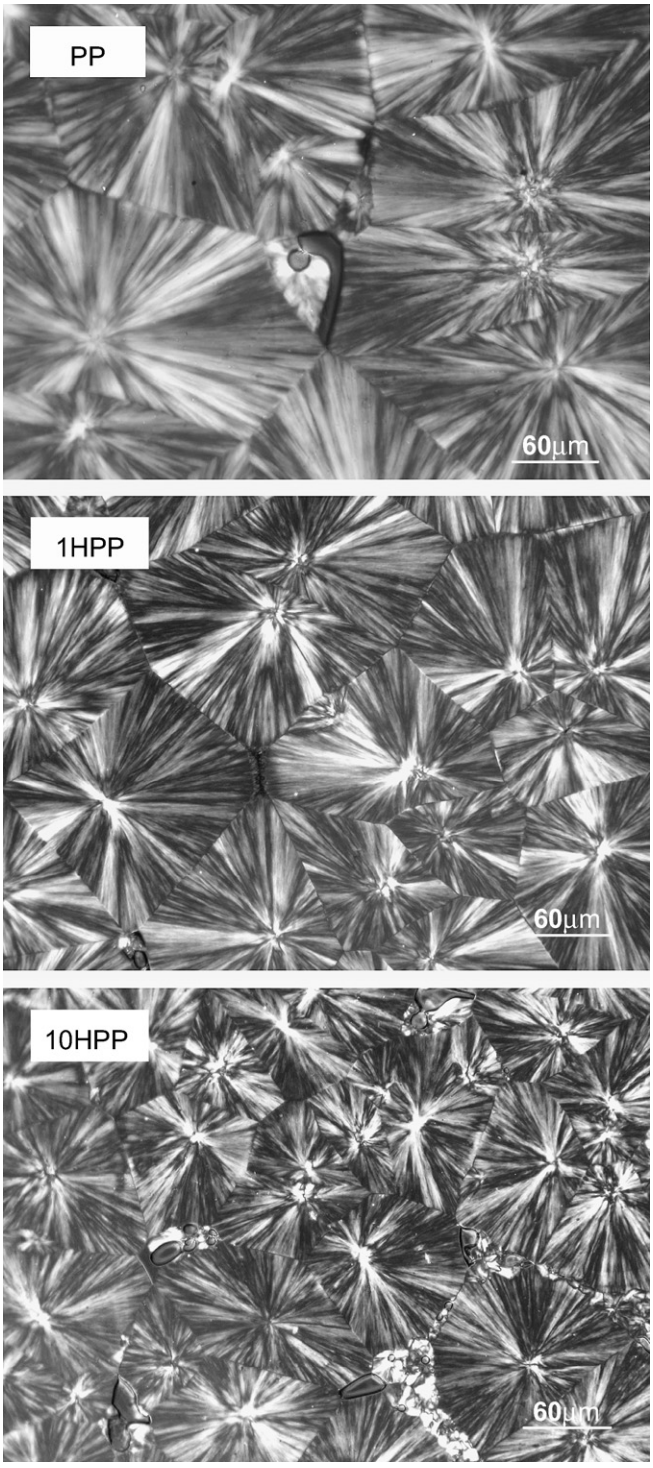


Fig. 9. The final crystal morphology of pure PP and PP/HNT composites crystallized at 128 °C.

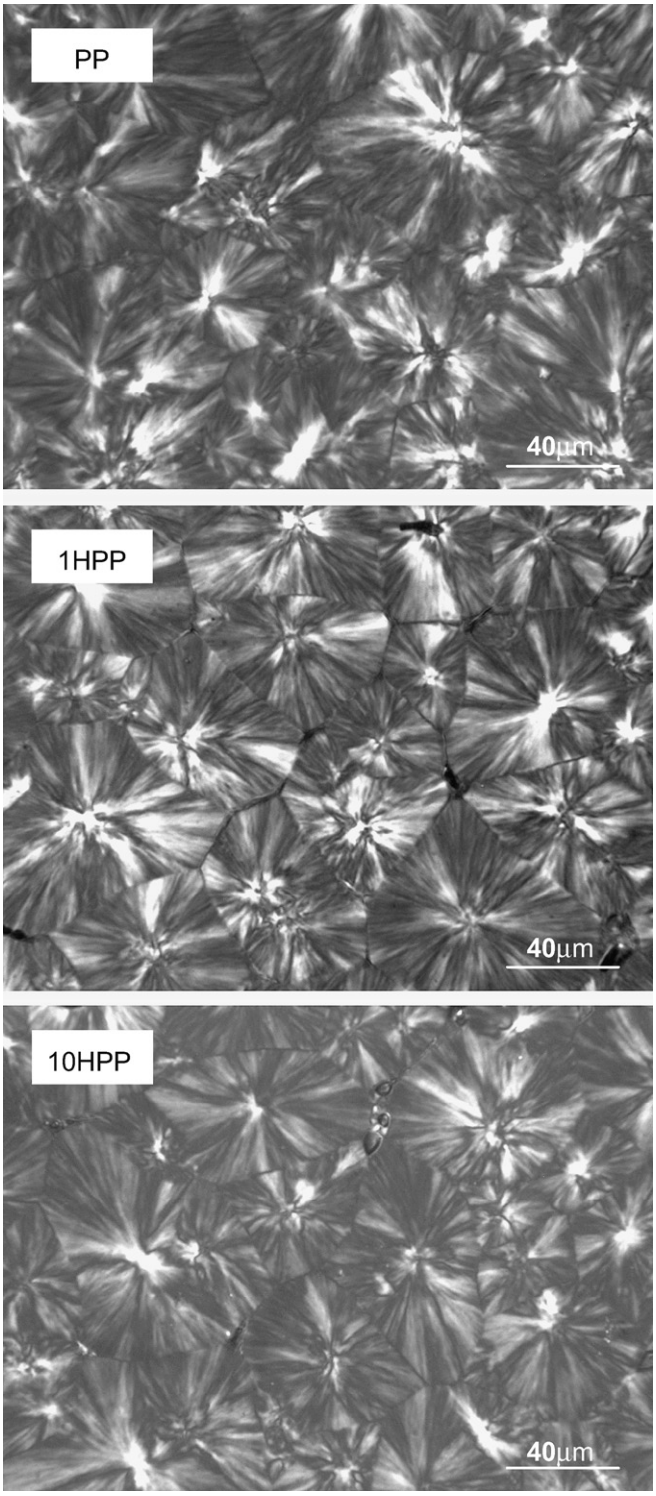


Fig. 10. The final non-isothermal crystal morphology of pure PP and PP/HNT composites (cooling rate: 50 °C/min).

grow to larger spherulites through fast nucleation and growth. One can also deduce that the homogeneous melt system changes into heterogeneous system in this period [38,39]. Thirdly, a level-off of $G'$ with time can be seen, which reveals that the system reaches an equilibrium and the crystallization process is over [39]. From Eq. (1), one can determine the half crystallization time $t_{1/2}$ when $\alpha(t) = 0.5$, which can be used to quantitatively evaluate the overall crystallization rate. The induction time and half crystallization time $t_{1/2}$ are summarized in Table 1. It can be clearly seen that $t_{1/2}$ value decreases by the addition of HNTs, mainly at a high level of HNTs. For example, the $t_{1/2}$ of pure PP is about 1750 s, which is decreased to only 660 s for 10HPP. It can be concluded that HNTs can serve as a heterogeneous nucleation agent and accelerate the

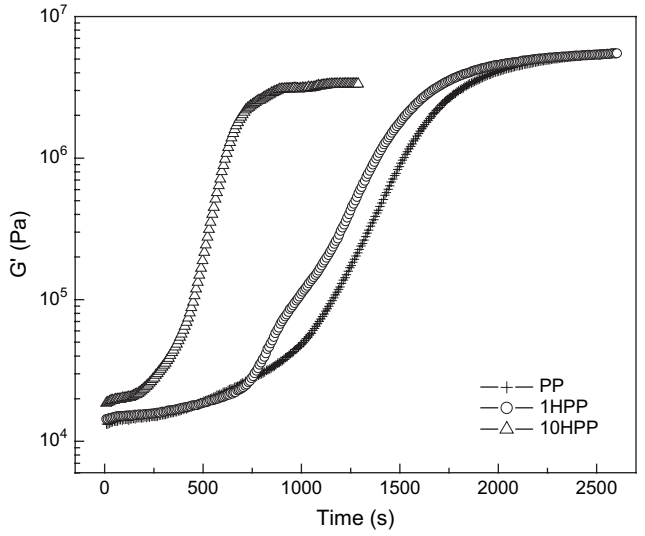


Fig. 11. Variation of the storage modulus ($G'$) with time of pure PP and PP/HNT composites at 1 Hz at isothermal crystallization temperature of 132 °C.

overall crystallization process of PP. The results are consistent well with the DSC observations. On the other hand, the induction time is seen to decrease with the increase of HNT content. For pure PP, the induction time is as long as 300 s, and this value decreases to 80 s for 10HPP. Obviously, the addition of HNTs has much more remarkable effect on the induction time than the half crystallization time $t_{1/2}$. As we know that the induction time represents the induction stage of nucleation and the half crystallization time $t_{1/2}$ represents the overall crystallization rate, including both nucleation and growth. The result obtained by dynamic melt rheometry indicates that HNTs mainly promote the nucleation and has not much influence on the growth of PP crystallization. These results are in good agreement with DSC and PLM observations.

### 3.5. WAXD analysis

WAXD analysis was performed to investigate the effect of HNTs on the crystalline structure of PP. Fig. 12 shows the X-ray diffractograms with the intensity as a function of the scattering angle, $2\theta$. One can see that five most intense WAXD reflections at $2\theta$ angles of 14.0°, 16.8°, 18.4°, 21° and 21.8°, corresponding to the (110), (040), (130), (111) and (041) lattice planes of the α-monoclinic crystalline structure of PP, appear in the X-ray diffraction spectra of each sample. This indicates that HNTs have no effect on PP crystal structure. One can also observe a peak at 12.02°, which is absent for pure PP but appears for the composites, corresponding to the 001 basal spacing of HNTs.

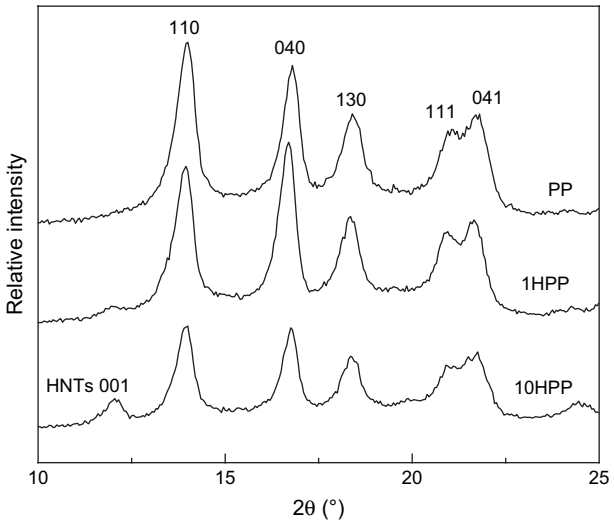


Fig. 12. WAXD curves of pure PP and PP/HNT composites.

The crystallinity of pure PP and PP/HNT composites can also be obtained from this WAXD intensity data, as shown in Table 1. It can be seen that the crystallinity of all the samples is almost the same, suggesting that the presence of HNTs has no obvious effect on the crystallinity of PP. This result is consistent well with the DSC result.

### 3.6. The mechanical properties of PP/HNT composites

Table 2 shows the mechanical properties of PP/HNT composites as well as pure PP. It can be seen that the tensile strength is not improved by the presence of HNTs, compared with pure PP. The impact strength of PP/HNTs is slightly increased from 2.6 kJ/m$^2$ to 3.3 kJ/m$^2$ as the HNT content increases to 10 wt% (10HPP).

## 4. Discussion

### 4.1. The effect of fillers on PP crystallization

Usually, the addition of nanofillers can largely enhance the crystallization rate and the crystallization temperature, and significantly decrease the spherulite size of PP. In Bhattacharyya's work [21], the presence of 0.8 wt% SWNTs remarkably increased the crystallization rate by as much as an order of magnitude, obviously enhanced the crystallization temperature by 11 °C and sharply decreased the spherulite size of PP. As reported by Chan et al. [14], an increase of 10 °C in the crystallization temperature and a significant decrease in spherulite

Table 1
Dynamic melt rheological data and crystallinity obtained by WAXD of PP/HNT composites as well as pure PP

| | PP | 1HPP | 10HPP |
|---|---|---|---|
| Induction time (s) | 300 | 220 | 80 |
| Half crystallization time (s) | 1750 | 1560 | 660 |
| Crystallinity (%) | 50.8 | 52.3 | 51.4 |

Table 2
Tensile strength and notched Izod impact strength of pure PP and PP/HNT composites

| | PP | 1HPP | 10HPP |
|---|---|---|---|
| Tensile strength (MPa) | 34.1 ± 0.3 | 36.4 ± 0.6 | 36.1 ± 0.5 |
| Notched Izod impact strength (kJ/m$^2$) | 2.6 ± 0.3 | 2.9 ± 0.2 | 3.3 ± 0.3 |

size of PP were achieved by the incorporation of $CaCO_3$ nanoparticles. In our earlier work [40], exfoliated clay layers were found serving as efficient nucleation agent for PP, resulting in a dramatic decrease in crystal size and an obvious increase of crystallization temperature and crystallization rate. In this work, although HNTs are well-dispersed in PP matrix in the range of 50–300 nm and have a good interfacial interaction with PP, the addition of HNTs can only enhance the crystallization temperature and overall crystallization rate of PP at a certain extent by acting as a not very good nucleation agent, which is different from the usual situations.

Furthermore, the effect of different kinds of fillers on the spherulite growth rate of PP varies. Some may retard the spherulite growth. For example, Nitta et al. [41] investigated the effect of silica particles on the spherulite growth rate of PP and observed that the growth rate decreased with increasing the silica content. Recently, the depressed spherulite growth rate of PP with the addition of $BaSO_4$ was observed by Wang et al. [42] due to the enhanced PP–$BaSO_4$ interaction promoting the particles to serve as physical crosslinking points. In our case, the addition of HNTs can enhance the nucleation and overall rate of PP crystallization, but has not much influence on the spherulite growth rate of PP. Similar reports can be found in literature. In Arroyo's work [18], a sensible increase of the overall crystallization rate was found by the presence of short glass fiber. However, it had no significant effect on the spherulite radial growth rate of PP. Canetti et al. [22] observed the same phenomenon in PP/lignin composites. Our work adds to this line, and indicates that nucleation and growth of a spherulite are two independent processes in PP/HNT composites.

### 4.2. Effect of HNTs on the mechanical properties of PP

From Table 2, the addition of HNTs shows no significant reinforcement for both tensile and impact strength of PP. It is well-known that the reinforcing effects of a kind of filler on the mechanical properties of polymer composites depend strongly on its shape, particles size, aggregate size, aspect ratio, surface characteristics and degree of dispersion [14]. In our work, not very much improved mechanical properties are observed for PP/HNT composites, although HNTs are dispersed in PP matrix uniformly for all the compositions prepared as shown in Fig. 2. Thus, the problem of agglomeration of nanofillers, which tends to decrease the mechanical properties of composites, does not exist. Furthermore, the interface of PP and HNTs is blurrier and no obvious cavities can be seen. From SEM photos of HNTs, we know that HNTs exhibit nanotubular structure and their length/diameter ratio ranges from 3 to 10. Most likely, the reinforcing effect of HNTs with such length/diameter ratio on mechanical properties of composites is limited. Therefore, this is one of the possible reasons that the mechanical properties of composites are not much improved, compared with other polymer composites. The length/diameter ratio may be further reduced after processing, due to the breaking of HNT particles under the shear effect. In addition, crystallinity and spherulite size have significant influence on the mechanical properties of crystalline polymer composites. In this work, both DSC and PLM results show that the nucleation effect of HNTs on PP crystallization is limited and the spherulite growth rate of composites is almost the same as pure PP, which can result in a roughly constant spherulite size by fast cooling, as shown in Fig. 10. Since the conditions of the samples' preparation (by injection molding) are very similar to the fast cooling, one can reasonably assume that the spherulite size in the injection molded samples is more or less the same. And also both DSC and WAXD results suggest a constant crystallinity in the samples. These can be the main reasons for the unchanged mechanical properties of PP/HNT composites of injection molded bars.

## 5. Conclusions

The crystallization behavior and mechanical properties of PP/HNT composites as well as pure PP are investigated. It is shown that HNTs are dispersed in PP matrix uniformly for all the compositions prepared, and can serve as a nucleation agent, resulting in an enhancement of the overall crystallization rate. On the other hand, a constant spherulite growth rate is observed at a given isothermal crystallization temperature, suggesting that nucleation and growth of a spherulite are two independent processes in the studied composites. Not much improvement of tensile and impact strength of PP/HNT composites of injection molded bars is observed by adding even 10 wt% of HNTs, and this could be mainly due to the constant crystallinity and unchanged spherulite size of PP as well as the small length/diameter ratio of HNTs.

## Acknowledgements

We would like to express our sincere thanks to the National Natural Science Foundation of China for financial support (50533050, 20634050 and 20490220). This work was subsidized by the special funds for Major State Basic Research Projects of China (2003CB615600).

## References

[1] Seo MK, Lee JR, Park SJ. Mater Sci Eng 2005;A404:79.
[2] Lin ZH, Peng M, Zheng Q. J Appl Polym Sci 2004;93:877.
[3] Zhang QX, Song JB, Wang SY, Mo ZS. Polymer 2005;46:11820.
[4] Kristiansen PM, Gress A, Smith P, Hanft D, Schmidt HW. Polymer 2006;47:249.
[5] Omonov TS, Harrats C, Groeninckx G. Polymer 2005;46:12322.
[6] Zhou XP, Xie XL, Yu ZZ, Mai YW. Polymer 2007;48:3555.
[7] Yazdani H, Morshedian J, Khonakdar HA. Polym Compos 2006;27:614.
[8] Zhao LJ, Li J, Guo SY, Du Q. Polymer 2006;47:2460.
[9] Ljungberg N, Cavaille JY, Heux L. Polymer 2006;47:6285.
[10] Fu SY, Lauke B, Mader E, Yue CY, Hu X. Compos Part A Appl Sci Manuf 2000;31:1117.
[11] Brandl W, Marginean G, Chirila V, Warschewski W. Carbon 2004;42:5.
[12] Wu CL, Zh MQ, Rong MZ, Friedrich K. Compos Sci Technol 2005;65:635.
[13] Gorga RE, Dondero Williams E. 2005 AIChE annual meeting and fall showcase. Conference proceedings: 2005. p. 13639.
[14] Chan CM, Wu JS, Li JX, Cheung Ying-Kit. Polymer 2002;43:2981.
[15] Liu YQ, Kontopoulou Marianna. Polymer 2006;47:7731.

[16] Weawkamol L, Minh-Tan TT, Florence PS. J Polym Sci Part B Polym Phys 2005;43:2445.
[17] Zhang Q, Fu Q, Jiang LX. Polym Int 2000;49:1561.
[18] Arroyo M, Lopez-Manchado MA. Polymer 1997;38:5587.
[19] Jian S, Goossens H, Duin MV. Polymer 2005;46:8805.
[20] Perrin-Sarazin F, Ton-That M-T, Bureau MN. Polymer 2005;46:11624.
[21] Bhattacharyya AR, Sreekumar TV, Liu T, Kumar S. Polymer 2003; 44:2373.
[22] Canetti M, Chirico AD, Audisio G. J Appl Polym Sci 2003;91:1435.
[23] Nitta KH, Asuka K, Liu BP, Terano M. Polymer 2006;47:6457.
[24] Nagasawa S, Fujimori A, Masuko T, Iguch M. Polymer 2005;46:5241.
[25] Noro H. Clay Miner 1986;21:401.
[26] Levis SR, Deasy PB. Int J Pharm 2002;243:125.
[27] Antill SJ. Aust J Chem 2003;56(7):723.
[28] Shchukin DG, Sukhorukov GB, Price RR, Lvov YM. Small 2005; 1(5):510.
[29] Wu JS. High impact strength from natural nanotubes. Third international symposium on engineering plastics, Urumqi, China; 2007.
[30] Du ML, Guo BC, Jia DM. Eur Polym J 2006;42:1362.
[31] Na B, Wang K, Zhang Q, Du RN, Fu Q. Polymer 2005;46:3190.
[32] Alexander LE. X-ray diffraction methods in polymer science. New York: Wiley-Interscience; 1969.
[33] Boutahar K, Carrot C, Guillet J. Macromolecules 1998;31:1921.
[34] Acierno S, Grizzuti N, Winter HH. Macromolecules 2002;35:5043.
[35] Pogodina NV, Winter HH. Macromolecules 1998;31:8164.
[36] Khanna YP. Macromolecules 1993;26:3639.
[37] Gauthier C, Chailan JF, Chauchard J. Macromol Chem 1992;193:1001.
[38] Yoon WJ, Myung HS, Kim BC, Im SS. Polymer 2000;41:4933.
[39] Dong WC, Kwang JK, Byoung CK. Polymer 2006;47:3609.
[40] Zhang Q, Gao XL, Wang K, Fu QC. J Polym Sci 2004;22:175.
[41] Nitta KH, Asuka KZ, Liu BP, Terano M. Polymer 2006;47:6457.
[42] Wang K, Wu JS, Zeng HM. Eur Polym J 2003;39:1647.